Drosophila Nedd4-long reduces Amphiphysin levels in muscles and leads to impaired T-tubule formation

Frozan Safi[a,b], Alina Shteiman-Kotler[a,b], Yunan Zhong[a,b], Konstantin G. Iliadi[a], Gabrielle L. Boulianne[a,c], and Daniela Rotin[a,b,*]

[a]Hospital for Sick Children, Toronto, ON M5G 0A4, Canada; [b]Biochemistry Department and [c]Molecular Genetics Department, University of Toronto, Toronto ON M5S 1A1, Canada

ABSTRACT ***Drosophila*** **Nedd4 (dNedd4) is a HECT ubiquitin ligase with two main splice isoforms: dNedd4-short (dNedd4S) and -long (dNedd4Lo). DNedd4Lo has a unique N-terminus containing a Pro-rich region. We previously showed that whereas dNedd4S promotes neuromuscular synaptogenesis, dNedd4Lo inhibits it and impairs larval locomotion. To delineate the cause of the impaired locomotion, we searched for binding partners to the N-terminal unique region of dNedd4Lo in larval lysates using mass spectrometry and identified Amphiphysin (dAmph). dAmph is a postsynaptic protein containing SH3-BAR domains and regulates muscle transverse tubule (T-tubule) formation in flies. We validated the interaction by coimmunoprecipitation and showed direct binding between dAmph-SH3 domain and dNedd4Lo N-terminus. Accordingly, dNedd4Lo was colocalized with dAmph postsynaptically and at muscle T-tubules. Moreover, expression of dNedd4Lo in muscle during embryonic development led to disappearance of dAmph and impaired T-tubule formation, phenocopying *amph*-null mutants. This effect was not seen in muscles expressing dNedd4S or a catalytically-inactive dNedd4Lo(C→A). We propose that dNedd4Lo destabilizes dAmph in muscles, leading to impaired T-tubule formation and muscle function.**

Monitoring Editor
Jeffrey D. Hardin
University of Wisconsin

Received: Jun 19, 2015
Revised: Jan 7, 2016
Accepted: Jan 15, 2016

INTRODUCTION

The *Drosophila melanogaster* larval body wall muscles are established during embryogenesis beginning with the invagination of the mesoderm, which spreads along the ectoderm and then forms numerous mesodermal derivatives (Dobi *et al.*, 2015). Somatic mesodermal specification produces three different types of myoblasts. Fusion of muscle founder cells and fusion-competent myoblasts form the syncytial myotube, which develops into the embryonic and larval body wall muscles (Dobi *et al.*, 2015). After myoblast fusion, nuclei are positioned correctly throughout the myotube (Folker and Baylies, 2013) and form connections to surrounding tendon cells to establish the myotendinous junction, which is innervated by motorneurons in a process called neuromuscular (NM) synaptogenesis (Landgraf *et al.*, 1999; Volk, 1999; Collins and DiAntonio, 2007). The contractile apparatus is then assembled, and muscles begin to contract. During larval stages, the essential muscle pattern created in the embryo does not change, except that the muscles continue to expand along with the growth of the larva (Dobi *et al.*, 2015). In *Drosophila* larva, a repeated pattern of 30 unique muscle fibers is present in each abdominal hemisegment (Bate, 1990), which are innervated by 36 motor neurons (Landgraf *et al.*, 2003). Each muscle fiber is distinguishable by size, shape, orientation, number of nuclei, innervation, and tendon attachment sites (Baylies *et al.*, 1998). Throughout development, internal and external cues guide muscles to adopt specific properties that allow them to perform particular functions.

Ubiquitination is the process of conjugating ubiquitin onto proteins, and it plays an important role in controlling protein degradation/stability, as well as in trafficking, sorting, and endocytosis of transmembrane proteins (Glickman and Ciechanover, 2002). The ubiquitination cascade involves three enzymes—E1, E2, and E3—with the last responsible for substrate recognition and ubiquitin

This article was published online ahead of print in MBoC in Press (http://www.molbiolcell.org/cgi/doi/10.1091/mbc.E15-06-0420) on January 28, 2016.
The authors declare no conflicting interests.

*Address correspondence to: Daniela Rotin (drotin@sickkids.ca).

Abbreviations used: Amph, Amphiphysin; Nedd4, neuronal precursor cell expressed developmentally down-regulated 4; T-tubule, transverse tubule.

transfer, either indirectly (e.g., RING E3 ligases) or directly (e.g., HECT E3 ligases; Rotin and Kumar, 2009).

Although many proteins are involved in the regulation of NM synaptogenesis in flies, the role of the ubiquitin system in this process is less well characterized. Studies have shown that the RING-family ubiquitin ligase complex Highwire (Wan *et al*., 2000) inhibits synapse formation and function by inhibiting the kinase Wallenda/DLK1, the activator of JNK (Tian and Wu, 2013), whereas the deubiquitinating enzyme Fat Facet (Faf; DiAntonio *et al*., 2001) targets Liquid Facet/Epsin and promotes synaptic growth (Bao *et al*., 2008; Tian and Wu, 2013).

Neuronal precursor cell expressed developmentally down-regulated 4 (Nedd4) family members belong to the HECT family of E3 ligases and contain a common C2-WW(n)-HECT domain architecture. *Drosophila* contains a single dNedd4 gene, which undergoes alternative splicing to produce several splice isoforms, including two prominent ones: dNedd4-short (dNedd4S) and dNedd4-long (dNedd4Lo). Differences between the two isoforms of dNedd4 include an alternate start codon site, resulting in a longer N-terminal region in dNedd4Lo, and an extra exon inserted between those encoding WW1 and WW2 domains (Zhong *et al*., 2011).

Previously we showed that dNedd4S promotes NM synaptogenesis in flies (Ing *et al*., 2007) by interacting and ubiquitinating Commissureless (Comm), which leads to endocytosis of Comm from the muscle surface, a step required for NM synaptogenesis (Wolf *et al*., 1998). Recently our lab showed that whereas dNedd4S is essential for proper NM synaptogenesis (Ing *et al*., 2007), dNedd4Lo inhibits it (Zhong *et al*., 2011). Of importance, dNedd4Lo also inhibited normal larval locomotion (Zhong *et al*., 2011). These adverse effects of dNedd4Lo were caused by unique N-terminal and Middle regions found in dNedd4Lo (and absent from dNedd4S) and required a functional HECT domain (Zhong *et al*., 2011). Of interest, during embryonic muscle development, dNedd4Lo expression is dramatically decreased, whereas that of dNedd4S remains relatively high (Zhong *et al*., 2011).

Because we observed that the muscle and synaptogenesis defects of dNedd4Lo larvae were not caused by altered phosphorylation of dNedd4Lo, dNedd4Lo-mediated inhibition of catalytic activity of dNedd4S, or diminished effects of dNedd4Lo on Comm endocytosis (Zhong *et al*., 2011), we suspected that dNedd4Lo might inhibit muscle development and/or function by interacting with other proteins via its unique regions.

Here we identified, using mass spectrometry, *Drosophila* Amphiphysin (dAmph) as a binding partner of the unique N-terminal region of dNedd4Lo. Amphiphysins are members of the BAR-SH3 domain–containing family of proteins. Mammalian amphiphysin Amph I is involved in endocytosis and synaptic vesicle recycling during neurotransmission by interacting with clathrin/dynamin (Lichte *et al*., 1992; Di Paolo *et al*., 2002). In contrast, both mammalian Amph IIb (Bin1) and its fly orthologue, dAmph, are postsynaptic, lack binding sites for clathrin/dynamin, and are not involved in endocytosis. Instead, Bin1 and dAmph regulate transverse tubule (T-tubule) biogenesis in muscles (Leventis *et al*., 2001; Razzaq *et al*., 2001; Zelhof *et al*., 2001; Lee *et al*., 2002; Muller *et al*., 2003; Al-Qusairi and Laporte, 2011).

We demonstrate here that the N-terminus of dNedd4Lo directly binds to dAmph-SH3 domain. In accord, dNedd4Lo and dAmph are colocalized postsynaptically at neuromuscular junctions (NMJs) and muscle transverse tubules (T-tubules). Our data show that dNedd4Lo regulates the levels of dAmph postsynaptically and in muscles. Moreover, expression of dNedd4Lo in muscles results in impaired T-tubule formation, phenocopying *amph*-null mutants. These results demonstrate an important role of dNedd4Lo in regulating T-tubule organization of *Drosophila* muscles.

RESULTS

DAmph interacts with dNedd4Lo

Previously we found that dNedd4S promotes NM synaptogenesis (Ing *et al*., 2007) but that dNedd4Lo negatively regulates this process and, of importance, inhibits muscle function (larval locomotion; Zhong *et al*., 2011). The unique N-terminal and Middle regions, as well as the HECT domain of dNedd4Lo, are involved in regulating these adverse effects (Zhong *et al*., 2011). Because these negative effects were not caused by inhibition (by dNedd4Lo) of the HECT domain of dNedd4S or by AKT phosphorylation of dNedd4Lo (Zhong *et al*., 2011), we suspected that the unique regions of dNedd4Lo might negatively regulate muscle function by interacting with other proteins. To identify such putative interacting partners, we incubated embryo lysates with purified (immobilized) unique regions of dNedd4Lo (N-terminus and Middle regions) and identified several high-confidence (>95%) interacting proteins by mass spectrometry (Supplemental Table S1). dAmph, which contains BAR and SH3 domains, was identified as a binding partner of the unique N-terminal region of dNedd4Lo (Supplemental Table S1 and Figure 1A). To validate the MS results, we tested whether dAmph can bind dNedd4Lo by coimmunoprecipitation (coIP). We transiently expressed hemagglutinin (HA)-tagged dAmph and Flag-tagged dNedd4Lo or dNedd4S in *Drosophila* S2 cells and found binding (coIP) of dAmph with dNedd4Lo but not dNedd4S (Figure 1B).

dNedd4Lo N-terminus directly binds to the SH3 domain of dAmph

dAmph contains a C-terminal SH3 domain, a domain that usually binds proline-rich motifs (Grabs *et al*., 1997). DNedd4Lo N-terminus contains a Pro-rich sequence with a perfect consensus motif for SH3 binding (PRPPPR). We therefore tested in vitro binding of a purified SH3 domain of dAmph to the purified N-terminus of dNedd4Lo. Purified histidine (His)-tagged full-length (wild-type [WT]) dAmph, SH3-domain deletion mutant (dAmph-Δ*SH3*), SH3 mutant (dAmph SH3(W→A) containing a mutation in the conserved Trp required for binding the Pro-rich motif), or the SH3 domain of dAmph alone (SH3 dAmph; Figure 2A) was incubated with purified glutathione *S*-transferase (GST)–tagged dNedd4Lo N-terminus (residues 1–63). WT dAmph and the dAmph-SH3 domain bound to GST-dNedd4Lo N-terminus, whereas the dAmph(Δ*SH3*) and dAmph-SH3(W→A) mutants did not (Figure 2B). This demonstrates that the SH3 domain of dAmph directly binds the N-terminus of dNedd4Lo.

dAmph colocalizes with dNedd4Lo in muscles and postsynaptically

dAmph is enriched postsynaptically at NMJs and muscle T-tubules (Leventis *et al*., 2001), and our earlier (Ing *et al*., 2007) and present (Supplemental Figure S1) work detected endogenous dNedd4 expression in larval muscles, including T-tubules and NMJs. To investigate the biological importance of the dAmph:dNedd4Lo interaction in vivo, we first analyzed colocalization of dAmph and dNedd4Lo in the postsynaptic region and the muscle T-tubule network. We previously showed that endogenous dAmph colocalizes with the postsynaptic marker Dlg at NMJs (Leventis *et al*., 2001). Here we overexpressed Flag-tagged dNedd4Lo and V5-tagged dAmph in flies using the muscle-specific driver *24B-Gal4* and examined larval NMJs located on muscles 6/7 by immunohistochemistry with antibodies against Flag (dNedd4Lo), V5 (dAmph), and horseradish peroxidase (HRP; presynaptic marker). DNedd4Lo colocalized with

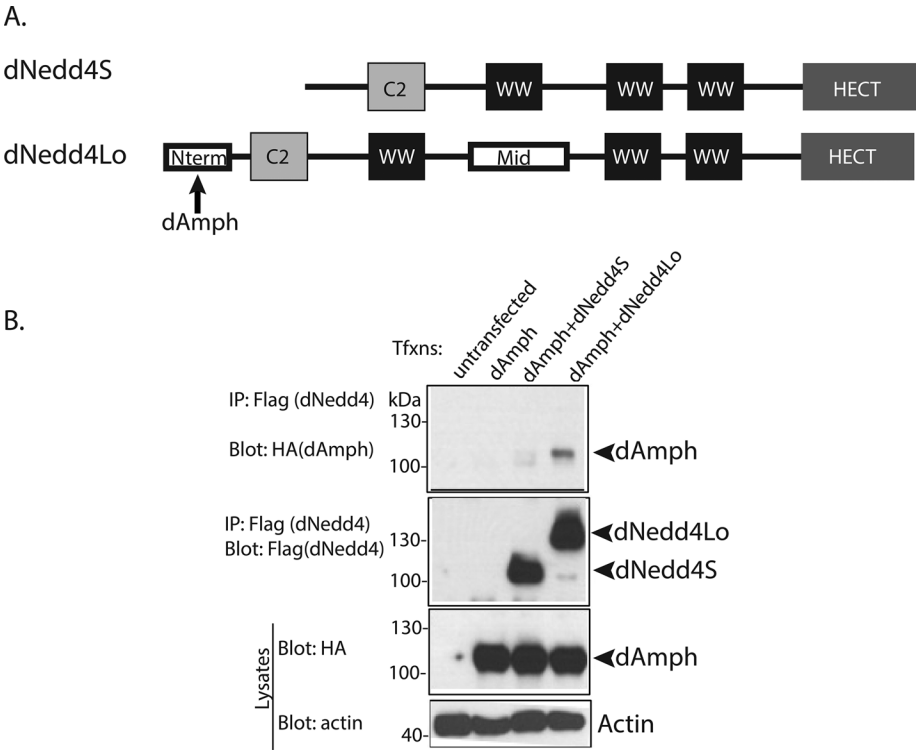

FIGURE 1: dNedd4Lo coimmunoprecipitates with dAmph. (A) Schematic representation of dNedd4S and dNedd4Lo, showing the C2, WW(x3), and HECT domains. DNedd4Lo contains unique N-terminal (Nterm) and Middle (Mid) regions that are absent in dNedd4S. The *Drosophila* Amphiphysin (dAmph) protein was identified as an interacting partner of the unique N-terminal region of dNedd4Lo by mass spectrometry. (B) DAmph binds to dNedd4Lo in *Drosophila* S2 cells. *Drosophila* S2 cells were transfected (Tfxn) with Flag-tagged dNedd4S or dNedd4Lo and HA-tagged dAmph. Transfected cells were lysed, and the lysates were immunoprecipitated (IP) with anti-Flag (dNedd4) antibodies and immunoblotted with anti-HA to detect coimmunoprecipitated dAmph (top). Second from top, precipitated Flag-dNedd4 proteins. Bottom, dAmph expression in the lysates were verified using anti-HA antibodies, and actin was used as a loading control.

dAmph in muscles but not with HRP labeling, which is specific for presynaptic neuronal membranes (Figure 3A). To verify that V5-dAmph is localized postsynaptically and in muscle T-tubules, we examined NMJs using antibodies against V5, HRP, and a postsynaptic/T-tubule marker, Disc large (Dlg; Figure 3B). Similar to what we previously observed with endogenous dAmph, V5-dAmph colocalized with Dlg labeling (Figure 3B), indicating that dNedd4Lo colocalizes with dAmph in the postsynaptic region and muscle T-tubules.

dAmph lacking its SH3 domain is mislocalized in muscles and no longer colocalizes with dNedd4

Because we found that the interaction between dNedd4Lo and dAmph is mediated by the SH3 domain of dAmph, we expect this interaction to be lost in vivo in *dAmph(ΔSH3)* mutant flies. To determine the localization of the *dAmph(ΔSH3)* mutant in *Drosophila*, we analyzed UAS transgenic fly lines that overexpress Myc-tagged dAmph(ΔSH3) in muscles. In contrast to WT dAmph, dAmph(ΔSH3) did not colocalize in muscle T-tubules with Dlg (Supplemental Figure S2, A and B) or with dNedd4 (Supplemental Figure S3, A and B). Deletion of the SH3 domain of dAmph shifts its localization from the muscle T-tubules and postsynaptic region to a region near the plasma membrane of the muscles (Supplemental Figure S2, A and B). Quantification of Pearson's *r* further shows that dAmph WT colocalizes with the postsynaptic marker Dlg (r = 0.83; Supplemental Figure S2C) but that the SH3-domain deletion mutant dAmph(ΔSH3) shows significantly reduced colocalization (r = 0.45). Similarly, Pearson's *r* for V5-dAmph (WT) colocalization with endogenous dNedd4 was 0.62 versus 0.32 for dAmph(ΔSH3 (Supplemental Figure S3C). These results indicate that the SH3 domain of dAmph is important for its localization in muscle T-tubules and the postsynaptic region of muscles.

DNedd4Lo regulates the levels of dAmph in the postsynaptic region

Because dNedd4Lo is an E3 ubiquitin ligase, we investigated the possibility that it regulates levels of dAmph in vivo in muscle, including the postsynapse. Thus we analyzed the levels of endogenous dAmph in our UAS transgenic fly lines, which overexpress dNedd4S, dNedd4Lo, and dNedd4Lo(C→A) (a catalytically inactive mutant generated by mutating the catalytic cysteine in the HECT domain to alanine). The flies used in this experiment have WT genetic background because *dNedd4*-null (*dNedd4*^{T121FS}) flies are homozygous lethal during embryogenesis and cannot be rescued with dNedd4Lo overexpression (Zhong *et al.*, 2011).

If dNedd4Lo regulates dAmph, then we would expect dAmph abundance in the muscle (see later discussion) and postsynaptic region to be reduced in flies overexpressing dNedd4Lo but not the dNedd4Lo(C→A) mutant or dNedd4S. We examined larval NMJs located on muscles 6/7 by immunohistochemistry with antibodies against dAmph and Dlg. *w*^{1118} flies (defined here as WT) and *damph*^{5E3} (*amph*-null) transgenic flies that have their entire *amph* gene deleted were used as controls (Leventis *et al.*, 2001). The mean intensity of dAmph in the postsynaptic region was used to quantify the levels of dAmph; Dlg labeling was used as a postsynaptic marker. Wild-type and dNedd4S flies show enrichment of dAmph in this area with the postsynaptic marker Dlg (Figure 4A, C and F). As expected, in *amph*-null flies, dAmph was not detected in the postsynaptic region (Figure 4, B and F). Of importance, in larvae overexpressing dNedd4Lo, dAmph levels were significantly reduced (Figure 4, D and F), whereas larvae overexpressing dNedd4Lo(C→A) show near-normal levels of dAmph (Figure 4, E and F).

Similar to endogenous dAmph, postsynaptic levels of V5-tagged dAmph were also reduced in the presence of dNedd4Lo (Supplemental Figure S4, C and E). In contrast, we did not observe any significant reduction in the levels of V5-tagged dAmph in the presence of dNedd4S or dNedd4Lo(C→A) (Supplemental Figure S4). Of interest, levels of the postsynaptic protein Dlg were also lower in flies overexpressing dNedd4Lo or in *amph*-null mutants but not dNedd4S- or dNedd4Lo(C→A)-expressing flies (Supplemental Figures S4 and S5). In contrast, expression of another postsynaptic protein, the glutamate

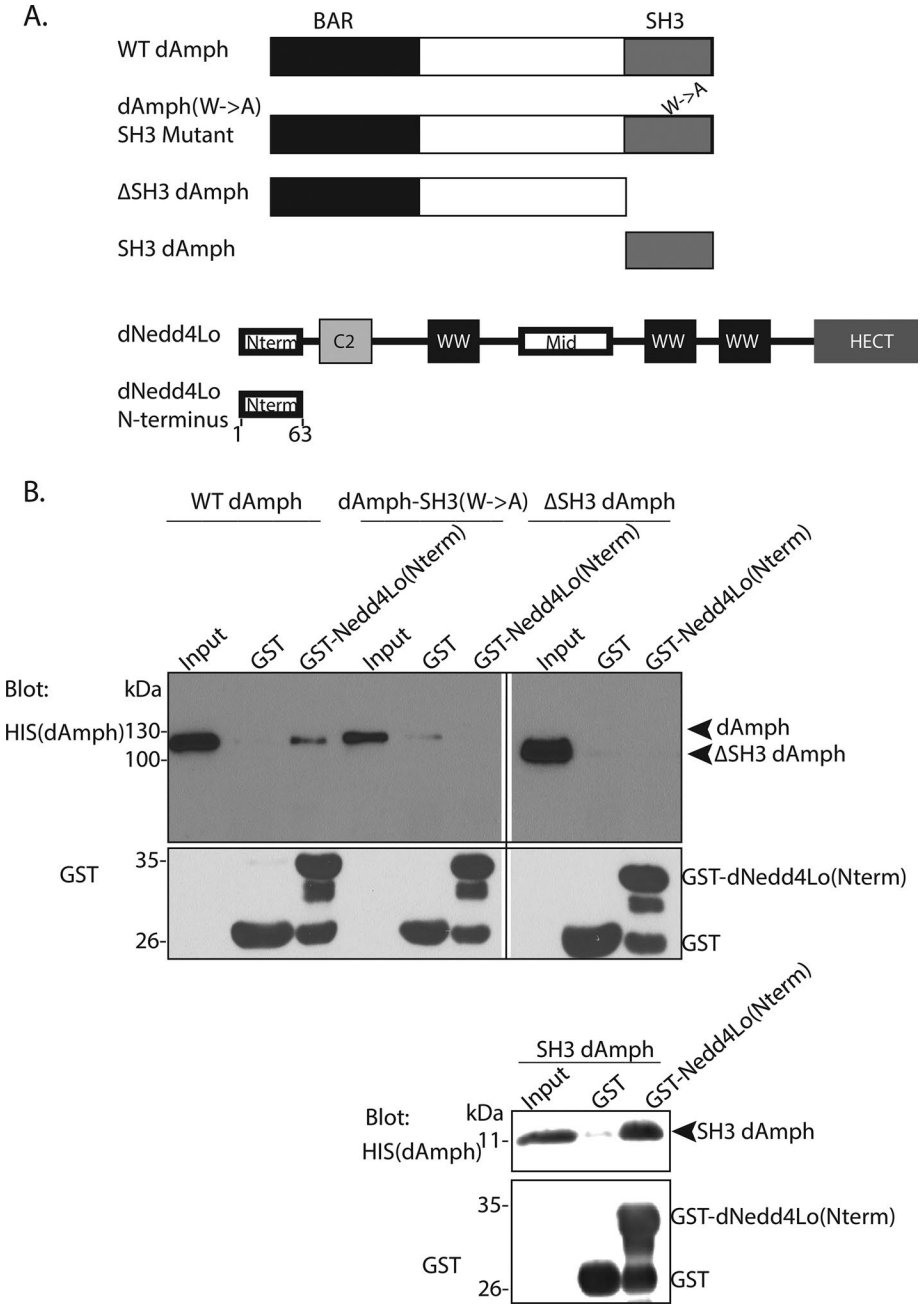

FIGURE 2: *Drosophila* Amphiphysin directly binds the N-terminus of dNedd4Lo via its SH3 domain. (A) Schematic representation of dNedd4Lo, the unique N-terminal region of dNedd4Lo (Nterm, residues 1–63), WT dAmph, the SH3 mutant containing a tryptophan-to-alanine substitution in the SH3 domain (dAmph SH3(W→A)), SH3 deletion mutant (ΔSH3 dAmph), and the SH3 domain alone (SH3 dAmph). (B) The SH3 domain of dAmph mediates direct binding to the N-terminal region of dNedd4Lo. His-tagged purified dAmph (WT, ΔSH3, SH3(W→A) or SH3 domain alone) was incubated with GST beads or GST fused to dNedd4Lo N-terminal region (GST dNedd4Lo(Nterm)). DAmph was detected using His antibodies and dNedd4Lo(Nterm) using GST antibodies.

receptor GluRII, was not affected by loss of *amph* (Supplemental Figure S6).

Collectively these results indicate that muscle-specific overexpression of dNedd4Lo reduces levels of dAmph in the postsynaptic region of the larval NMJ, an effect that requires the catalytic activity of dNedd4Lo.

DNedd4Lo regulates the organization of muscle T-tubules

In *Drosophila* muscles, T-tubules run longitudinally along the muscle fiber and cross the sarcomere transversely (Figure 5A). Previous studies showed that dAmph is localized on T-tubules and can tubulate membranes (Razzaq *et al.*, 2001). Furthermore, *amph*-null mutants exhibit a severely disorganized sarcoplasmic reticulum system, lacking T-tubules (Razzaq *et al.*, 2001). Because dNedd4Lo overexpression significantly reduced the levels of dAmph in the postsynaptic membrane, we postulated that dNedd4Lo might also be involved in regulating dAmph in muscle T-tubules. We thus examined larval T-tubules located on muscles 6/7 by immunohistochemistry with antibodies against dAmph and Dlg (T-tubule marker) in UAS transgenic fly lines overexpressing dNedd4S, dNedd4Lo, or dNedd4Lo(C→A) in the muscles. We used *amph*-null mutants as a control to visualize the disorganized T-tubule phenotype of flies lacking dAmph. As expected, in *amph*-null mutant larvae, Dlg staining revealed that loss of dAmph results in severe disorganization and reduction of the T-tubule network. Specifically, transverse tubules are lost, and the remaining tubules are predominantly longitudinal and sometimes broader (Figure 5, C and G). Wild-type and dNedd4S larvae consistently show a high degree of T-tubule branching from longitudinal tubules (Figure 5, B and D). Of interest, Dlg staining showed that dNedd4Lo overexpression significantly reduced the number of transverse tubules but did not affect the number of longitudinal ones, similar to the *amph*-null mutant (Figure 5, E and H). In contrast, dNedd4Lo(C→A) overexpression, like dNedd4S and WT, consistently showed normal transverse tubules branching from longitudinal tubules (Figure 5F). We first quantified the T-tubule defect by analyzing ~30–80 hemisegments of each larva and comparing it to WT to determine whether segments appeared normal or abnormal. Flies overexpressing dNedd4Lo show a significantly higher percentage of abnormal muscle segments relative to WT flies (Figure 5I). We also counted the T-tubules that appeared to branch from a longitudinal tubule segment to determine whether there was a specific effect on the number of T-tubules present; when dNedd4Lo was overexpressed in muscles, there was a significant decrease in the number of T-tubules, similar to *amph*-null mutants (Figure 5J). These results indicate that dNedd4Lo is involved in regulating the organization of the T-tubule network in larval muscles, likely by reducing levels of dAmph.

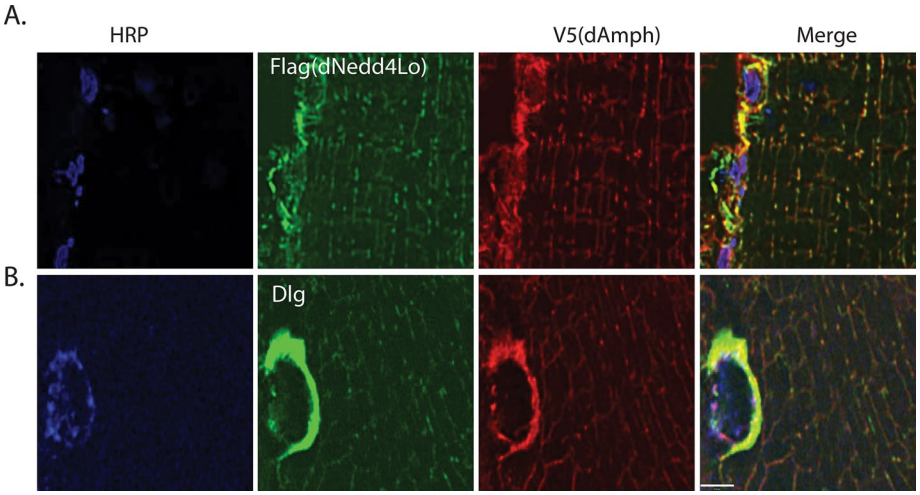

FIGURE 3: *Drosophila* Amph and dNedd4 are enriched postsynaptically at the neuromuscular junctions and muscle T-tubules. (A) DNedd4Lo is expressed in the muscles and the postsynaptic region of the NMJ, where it colocalizes with dAmph. (B) DAmph is enriched postsynaptically in NMJs and muscle T-tubules, where it colocalizes with postsynaptic and T-tubule marker Dlg. Expression was driven by *24B-Gal4* in larval muscles, dNedd4Lo (UAS-*dNedd4Lo*) was detected with an anti-Flag antibody (green), and dAmph (*UAS-V5-dAmph)* was detected with V5 antibody (red). Synaptic boutons from muscles 6/7 were analyzed. Presynaptic marker: HRP (blue). Scale bar, 3 μm. The image depicts a single optical section.

dAmph protein levels in the muscle are reduced in flies overexpressing dNedd4Lo

Because dNedd4Lo overexpression caused a significant decrease in the number of T-tubules, which mimics the *amph*-null phenotype, we hypothesized that dAmph protein levels in the muscles might be reduced by dNedd4Lo. Thus we examined the levels of dAmph in muscles isolated from flies overexpressing Flag-tagged dNedd4S, dNedd4Lo, or dNedd4Lo(C→A). Our results (Figure 6, A and B) show that flies overexpressing dNedd4Lo have lower levels of dAmph in the muscle relative to WT. In contrast, flies overexpressing dNedd4S have normal levels of dAmph (Figure 6, A and B). Although flies expressing the catalytically inactive dNedd4Lo(C→A) revealed somewhat lower levels of dAmph than WT, these differences were not statistically significant ($p = 0.063$; Figure 6, A and B). Similar to endogenous dAmph, in flies overexpressing both V5-tagged dAmph and Flag-dNedd4, the level of overexpressed dAmph was strongly reduced in muscles of dNedd4Lo-expressing flies but not in those expressing dNedd4S or dNedd4Lo(C→A) (Figure 6C).

Genetic interactions between dAmph and dNedd4Lo reduce larval locomotion

We previously showed that *amph*-null larvae, as well as dNedd4Lo-overexpressing larvae, exhibit impaired locomotion (Leventis *et al.*, 2001; Zhong *et al.*, 2011), as also shown in Figure 7. To test for genetic interactions between dAmph and dNedd4Lo, we crossed the *amph*-null flies to dNedd4Lo-overexpressing flies and analyzed the locomotor activity of the resultant dAmph(+/–);dNedd4Lo larvae. This led to a further significant impairment in locomotor activity of the dAmph(+/–);dNedd4Lo larvae relative to either dAmph(+/–) ($p < 0.001$) or dNedd4Lo-overexpressing larvae alone ($p = 0.025$; Figure 7B), suggesting genetic interactions between dAmph and dNedd4Lo.

DISCUSSION

We previously showed that unlike dNedd4 (dNedd4S), muscle-specific overexpression of the dNedd4Lo isoform inhibits NM synaptogenesis and leads to impaired larval locomotion and lethality (Zhong *et al.*, 2011). This effect required the catalytic activity of dNedd4Lo, since a mutant dNedd4Lo(C→A) with an inactivating mutation in the HECT domain (Cys → Ala) was not inhibitory. This suggested that the same gene (dNedd4) can encode isoforms with opposite functions. In accord with this, we observed that during stages of embryonic development when synaptogenesis takes place (14–24 h), dNedd4S expression remains relatively high, whereas that of the inhibitory dNedd4Lo is strongly reduced (Zhong *et al.*, 2011), suggesting tight regulation of expression of these isoforms to promote muscle development at a very precise time. The inhibitory effect of dNedd4Lo is mediated by two regions unique to dNedd4Lo (N-terminus and Middle region), as deletion of these unique regions alleviated the synaptogenesis defects and increased viability (Zhong *et al.*, 2011). Therefore we postulated that the unique regions of dNedd4Lo might negatively regulate NM synaptogenesis and muscle development by targeting specific substrate(s).

Here we identified dAmph as a binding partner for the unique N-terminal region of dNedd4Lo by mass spectrometry and validated the interaction in vitro and in vivo in flies. We showed that transiently expressed dAmph coimmunoprecipitates with dNedd4Lo but not with dNedd4S in *Drosophila* S2 cells and demonstrated direct binding between dAmph-SH3 domain and the dNedd4Lo N-terminus. Our in vivo results showed that dAmph colocalizes with dNedd4Lo postsynaptically at neuromuscular junctions and muscle T-tubules, where their expression overlaps with the postsynaptic/T-tubule marker, Dlg. Of importance, we demonstrate that dNedd4Lo expression significantly reduced the levels of dAmph in the postsynaptic region and muscles, an effect not observed in larvae expressing dNedd4S or dNedd4Lo(C→A). As expected, due to the disappearance of endogenous dAmph in larvae expressing dNedd4Lo (and the inability to "treat" live larvae with proteasome inhibitors), we were not able to detect ubiquitination of dAmph in these larvae. In addition to biochemical interactions, we also show genetic interactions between dNedd4Lo and dAmph.

The reduction in dAmph levels in the dNedd4Lo-expressing muscles correlated with impaired T-tubule formation, mimicking the phenotype of the *amph*-null flies. These results could help explain (along with our previously described NM synaptogenesis defects; Zhong *et al.*, 2011) our observed locomotion defects in the dNedd4Lo-overexpressing larvae. At present, we cannot quantify the contribution of the T-tubule defects versus the NM synaptogenesis defects to the impaired muscle locomotion/function.

Interestingly, we found that flies overexpressing the dAmph(ΔSH3) mutant in muscles showed reduced localization at the postsynaptic region and T-tubules and no longer colocalized with dNedd4. It is known that the SH3 domain of some membrane-associated proteins is important for their targeting to specific subcellular locations (Bar-Sagi *et al.*, 1993). Similarly, we found that the SH3 domain of dAmph is also important for its location in the postsynaptic region and the muscle, since the ΔSH3 dAmph protein mislocalized to a region near the muscle plasma membrane. We do not know whether this SH3-dependent localization is related to the ability of

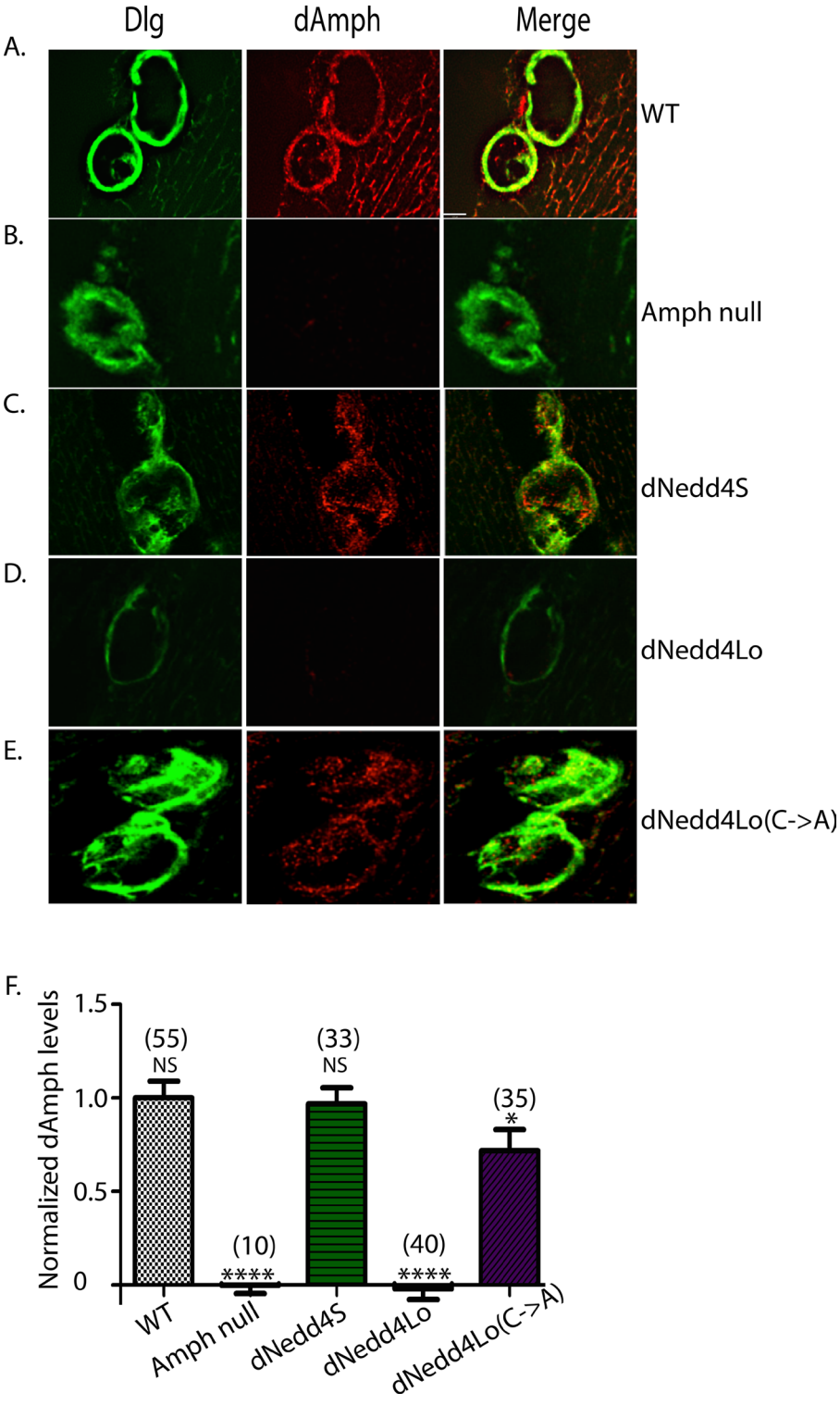

FIGURE 4: Postsynaptic levels of dAmph are significantly reduced in *Drosophila* muscles overexpressing dNedd4Lo. (A) Muscle driver control line *(+/24B-Gal4)* shows the normal localization of dAmph with the postsynaptic marker Dlg. (B) Absence of dAmph in the synapse of the *amph*-null flies (negative control). (C–E) DAmph and Dlg expression in the postsynaptic region (muscles 6 and 7 are shown) of third-instar larvae overexpressing Flag-tagged (C) dNedd4S (UAS-*dNedd4S/24B-Gal4*), (D) dNedd4Lo (UAS-*dNedd4Lo/24B-Gal4*), or (E) dNedd4Lo(C→A) (UAS-*dNedd4Lo CA/24B-Gal4*), which were stained with anti-dAmph (red) and anti-Dlg (green) antibodies. Scale bar, 3 µm. (F) Quantification of levels of dAmph in the postsynaptic region. The postsynaptic region was identified as the area marked by Dlg labeling, and the intensity of dAmph in this region was measured. Numbers in the parentheses denote number of boutons analyzed. NS, not significant; *$p = 0.032$, ****$p < 0.0001$ (Student's *t* test).

this domain to bind dNedd4Lo or due to its interaction(s) with other molecules.

Amphiphysin has been implicated in T-tubule biogenesis (Lee *et al.*, 2002; Caldwell *et al.*, 2014; Lipsett *et al.*, 2015) due to its N-terminal amphipathic helix and BAR domain (N-BAR), which promotes membrane curvature (Peter *et al.*, 2004). The BAR domain of the isoform of mammalian amphiphysin 2 (Bin1) is known to be associated with T-tubule formation in skeletal and cardiac muscles (Caldwell *et al.*, 2014; Lipsett *et al.*, 2015), where it induces tubular plasma membrane invaginations (Lee *et al.*, 2002). Similar to Bin1, dAmph was shown to participate in plasma membrane remodeling during cleavage furrow ingression, which is required for de novo formation of cells in the *Drosophila* embryo; the BAR domain of dAmph is required for the formation of endocytic tubules that form at the cleavage furrow tips (Su *et al.*, 2013). Here we show that dNedd4Lo expression reduces the levels of dAmph in the muscle and significantly inhibits T-tubule formation. The degradation of dAmph by dNedd4Lo could impair T-tubule biogenesis by the BAR domain of dAmph, which could help to explain the larval locomotion defects we observed.

Cardiac Bin1 has been implicated in calcium channel trafficking and formation of the inner membrane folds of the cardiac T-tubules (Hong *et al.*, 2014; Lipsett *et al.*, 2015). Bin1 localizes to cardiac T-tubules with the L-type calcium channel, Cav1.2, by tethering dynamic microtubules to membrane scaffolds, allowing targeted delivery of Cav1.2 to cardiac T-tubules (Hong *et al.*, 2010). Knockdown of Bin1 reduces surface Cav1.2 and delays development of the calcium transient (Hong *et al.*, 2010). In cardiomyopathy, decrease in Bin1 alters T-tubule morphology and can cause arrhythmia (Hong *et al.*, 2014). Mice with cardiac *Bin1* deletion show decreased T-tubule folding, which leads to free diffusion of local extracellular ions, prolonging action-potential duration and increasing susceptibility to arrhythmias (Hong *et al.*, 2014). Bin1 is also important for maintenance of intact T-tubule structure and Ca^{2+} homeostasis in adult skeletal muscle (Tjondrokoesoemo *et al.*, 2011). Adult mouse skeletal muscles with Bin1 knockdown display swollen T-tubule structures, alterations to intracellular Ca^{2+} release, and compromised coupling between the voltage-gated calcium channel, dihydropyridine receptor (DHPR), and the intracellular calcium channel, ryanodine receptor 1 (Tjondrokoesoemo *et al.*, 2011).

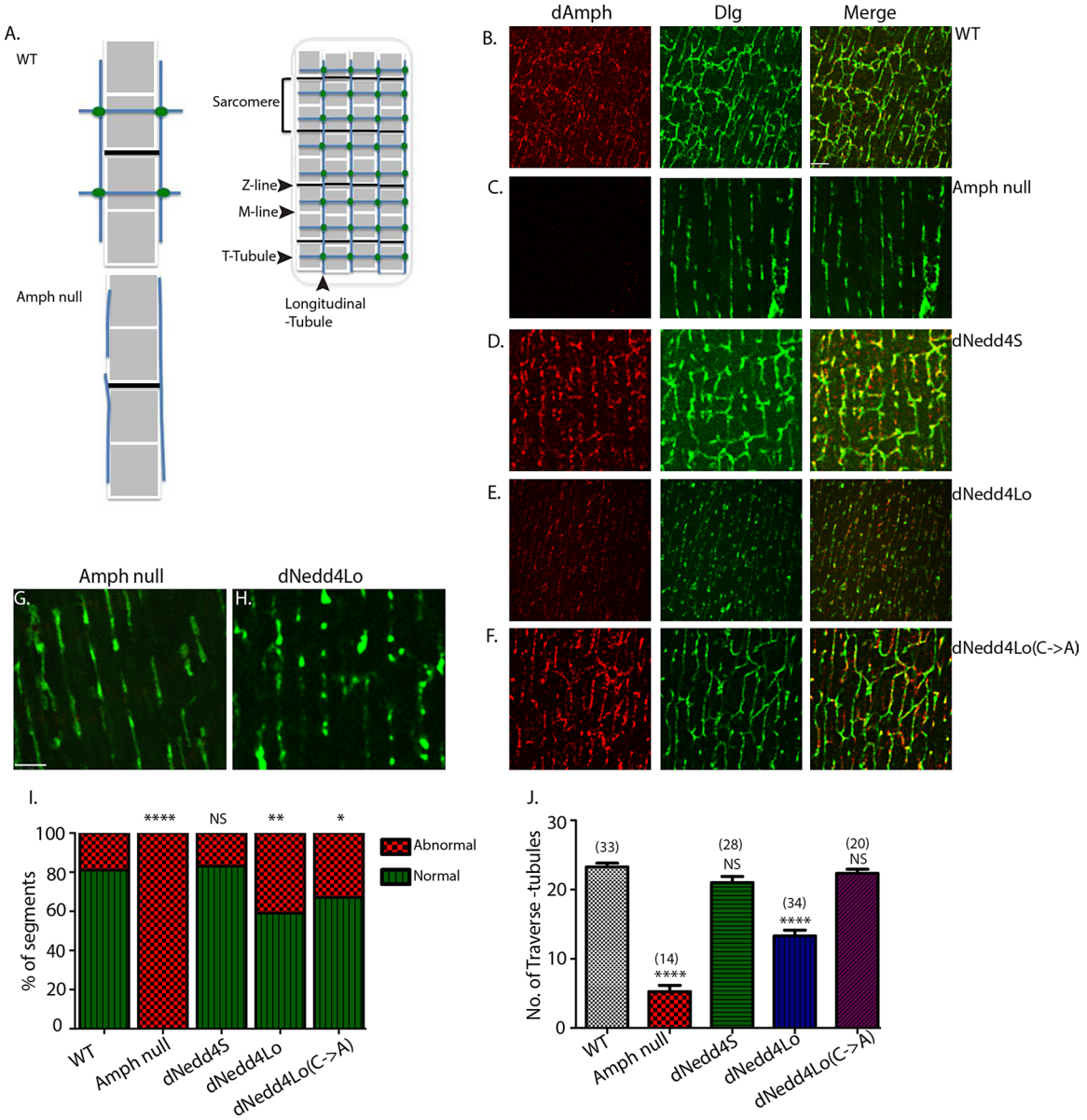

FIGURE 5: Overexpression of dNedd4Lo in muscles impairs the transverse tubule network. (A) Schematic representation of T-tubule staining in *Drosophila* muscles. In *Drosophila* muscles, T-tubules (green) run longitudinally along the muscle fiber and cross the sarcomere transversely. The WT T-tubule forms a box-like configuration with transverse (T) and longitudinal tubules (top). In *Amph-null* flies, the box-like configuration is lost, T-tubules are absent, and longitudinal elements are expanded. (B) Muscle driver control line (*+/24B-Gal4)* was included to show the normal T-tubule organization of the muscle with the T-tubule marker Dlg. (C) *Amph-null* flies were used as negative control to show absence of T-tubules and expanded longitudinal tubules. (D–F) DAmph and Dlg localization in the muscles (muscles 6 and 7 are shown) of third-instar larvae overexpressing (D) dNedd4S (UAS-*dNedd4S/24B-Gal4*), (E) dNedd4Lo (UAS-*dNedd4Lo/24B-Gal4*), or (F) dNedd4Lo(C→A) (UAS-*dNedd4Lo(C→A)/24B-Gal4*), which were stained with anti-dAmph (red) and Dlg antibodies (green). In E, muscle-specific overexpression of UAS-dNedd4Lo (*dNedd4Lo/24B-Gal4*) leads to T-tubule defects in muscles. (G, H) Higher magnification of the muscle T-tubules stained with the marker Dlg of (G) *amph*-null and (H) dNedd4Lo-overexpressing flies. Scale bars, 3 µm. (I) Quantification of the percentage of abnormal muscle segments in third-instar larval muscles from flies overexpressing dNedd4S (UAS-*dNedd4S/24B-Gal4*), dNedd4Lo (UAS-*dNedd4Lo/24B-Gal4*), or dNedd4Lo(C→A) (UAS-*dNedd4LoCA/24B-Gal4*), which were labeled with anti-Dlg antibodies. Muscle segments were scored (abnormal or normal) relative to muscles from WT flies. *$p = 0.0355$, **$p < 0.02$, ****$p < 0.0001$ (two-tailed Fisher's exact test). (J) Quantification of T-tubule branches in *Drosophila* larval muscles 6/7. The T-tubule branches along a segment of longitudinal tubule were counted in each muscle hemisegment. Numbers in parentheses denote the number of segments scored. ****$p < 0.0001$ (Student's *t* test). NS, not significant.

Similar to Bin1, dAmph is also required for the organization of the excitation-contraction coupling machinery of muscle (Razzaq *et al.*, 2001). Accordingly, *dAmph* mutant larvae and flies show defects in T-tubule formation, severe locomotor defects, and flight impairments, indicative of defects in muscle function (Leventis *et al.*, 2001; Razzaq *et al.*, 2001). Therefore degradation of dAmph in the

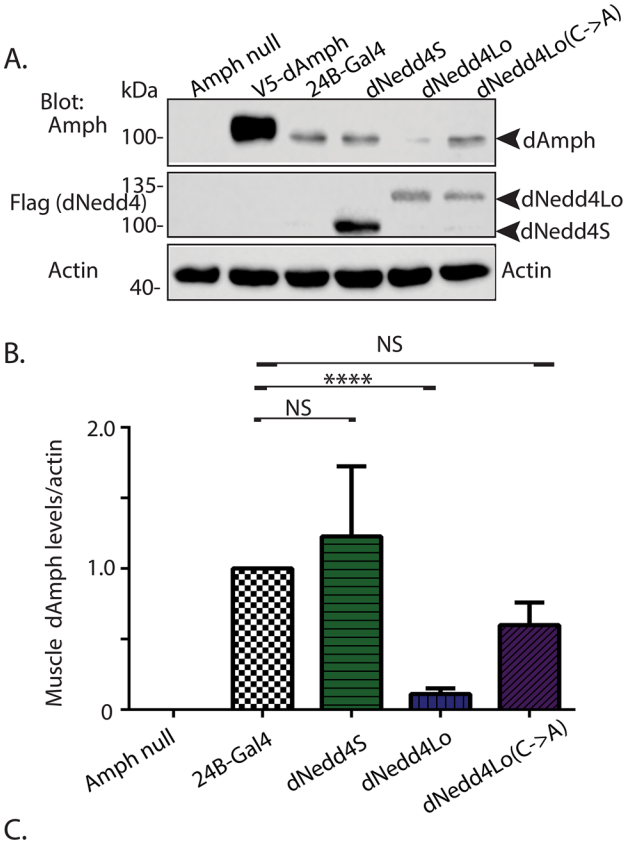

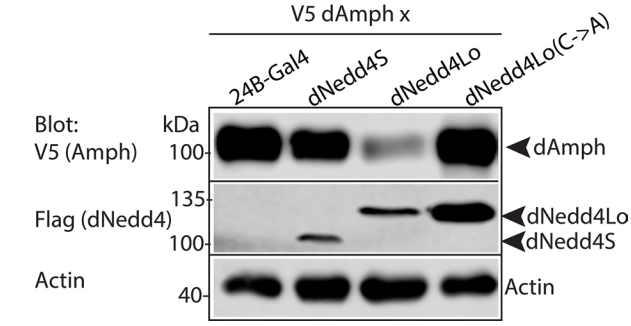

FIGURE 6: Muscle protein levels of dAmph are reduced in flies overexpressing dNedd4Lo. (A) Lysates from ~35 third-instar larvae (per genotype) overexpressing Flag-tagged dNedd4S (*UAS-dNedd4S/+; +/24B-Gal4*), dNedd4Lo (UAS-*dNedd4Lo/+;+/24B-Gal4*), or dNedd4Lo(C→A) (UAS-*dNedd4Lo(C→A)/+;+/24B-Gal4*) were collected. Levels of endogenous dAmph in each cross were analyzed using dAmph antibodies (top). Muscle driver control line (*+/24B-Gal4*) and V5-tagged dAmph (UAS-*dAmph/24B-Gal4*) were included to show the endogenous and overexpressed levels of dAmph in muscles, respectively. *Amph null* was used to show specificity of the dAmph antibodies. DNedd4 expression levels in the lysates were verified using anti-Flag antibodies; actin was used as a loading control (bottom). (B) Quantification of dAmph protein levels in muscles. The signal for dAmph in muscles was measured relative to actin level minus the signal from *amph* null to eliminate background. ****$p < 0.0001$ (Student's *t*-test, three independent experiments). NS, not significant. (C) Lysates from ~10 third-instar larvae (per genotype) overexpressing V5-tagged dAmph and Flag-tagged dNedd4S (*UAS-dNedd4S/+; UAS-dAmph/24B-Gal4*), dNedd4Lo (UAS-*dNedd4Lo/+;UAS-dAmph/24B-Gal4*), or dNedd4Lo(C→A) (UAS-*dNedd4Lo(C→A)/+;UAS-dAmph/24B-Gal4*) were collected. Expression of dAmph in each cross was analyzed using V5 antibodies (top). Muscle driver control line (*UAS-dAmph/24B-Gal4*) was included to show levels of overexpressed dAmph in muscles. DNedd4 expression levels in the lysates were verified using anti-Flag antibodies; actin was used as a loading control (bottom).

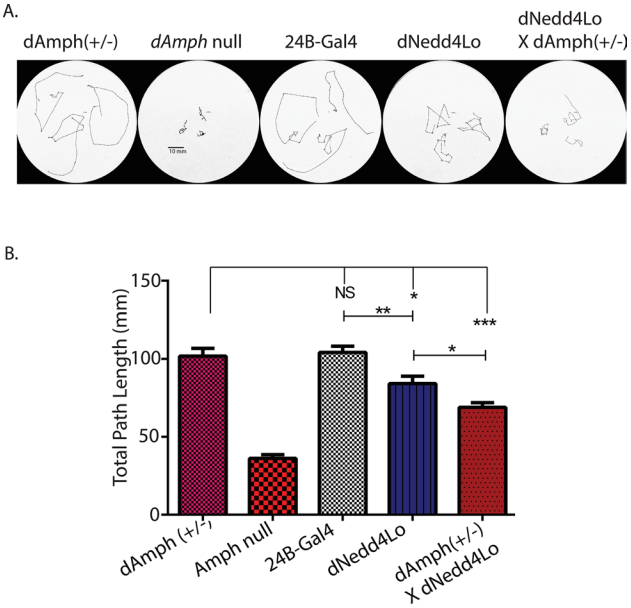

FIGURE 7: Genetic interactions between dAmph and dNedd4Lo reduce larval locomotion. *amph*-null flies were crossed to dNedd4Lo-overexpressing flies in muscles (dNedd4Lo;24B-Gal4) and analyzed for locomotor activity of the resultant dAmph(+/–);dNedd4Lo larvae. (A) Examples of larval walking path/traces. Bar, 10 mm. (B) Quantification of total path length of the indicated larvae. NS, Not significant. *$p = 0.025$, **$p = 0.009$, and ***$p < 0.001$.

muscle and inhibition of T-tubule biogenesis by dNedd4Lo could have adverse effects on the localization of T-tubule–associated calcium channels and coupling between the DHPR and ryanodine receptor, as a result altering calcium signaling in muscles. Efficient intracellular Ca^{2+} homeostasis in skeletal muscle requires intact triad junctional complexes comprising T-tubule invaginations of plasma membrane and terminal cisternae of sarcoplasmic reticulum. Because dNedd4Lo expression significantly reduced T-tubule projections, this would likely impair intracellular Ca^{2+} homeostasis and result in locomotor defects.

Although there is no direct homologue of dNedd4Lo in species other than *Drosophila*, the mammalian Nedd4 relative Itch has a proline-rich N-terminal region that binds the SH3 domain of Sorting Nexin 9 (Baumann *et al.*, 2010). In yeast, Rsp5 (the yeast orthologue of Nedd4 proteins) regulates the Amphiphysin homologue Rvs167 by monoubiquitination of lysine in the SH3 domain of Amphiphysin (Stamenova *et al.*, 2004), demonstrating that Nedd4 family members can interact with SH3 domains, including that of amphiphysin, in other species in addition to flies.

In addition to dAmph, we identified several other interacting partners of the N-terminal and Middle regions of dNedd4Lo that could potentially be targeted by dNedd4Lo. Similar to dAmph, two of these proteins, Syndapin (which, like dAmph, bound the unique N-terminus region of dNedd4Lo), and Sorting Nexin 9 (SH3PX1, which bound the unique Middle region of dNedd4Lo), contain BAR and SH3 domains. We also identified the SH3 domain–containing protein Cindr/CG31012 (orthologue of the

mammalian Cd2ap and Cin85) as a binding partner to the unique N-terminus of dNedd4Lo. We do not know whether these proteins are bone fide substrates of dNedd4Lo or contribute to the NMJ and T-tubule defects caused by overexpression of dNedd4Lo in the muscle during development.

In conclusion, the severely reduced locomotion activity of larvae overexpressing dNedd4Lo in the muscle may be explained by both impaired neuromuscular synaptogenesis, which we demonstrated previously (Zhong *et al.*, 2011), and by impaired T-tubule formation as a result of dAmph degradation by dNedd4Lo, which we show here. The defective T-tubule branching would likely impair coupling between the DHPR and ryanodine receptor, possibly by affecting the localization of calcium channels to the T-tubule network. Reduced surface calcium channels on the T-tubule network would alter calcium homeostasis and compromise excitation and contraction coupling, causing larval locomotor defects.

MATERIALS AND METHODS

Fly stocks

Fly strains and crosses are listed in Supplemental Table S3. Flies were maintained at room temperature on standard *Drosophila* medium. All experiments were performed at 25°C. All flies used in this experiment have a WT genetic background because *dNedd4*-null (*dNedd4*^{T121FS} homozygote) flies are homozygous lethal at the embryonic stage and cannot be rescued with dNedd4Lo overexpression (Zhong *et al.*, 2011).

Constructs

For generation of N-terminal and Middle unique sequences of dNedd4Lo, GST-tagged *dNedd4Lo* N-terminus (Nterm, residues 1–63) and *dNedd4Lo* Middle (Mid, residues 304–473) regions were subcloned into the pQE30 vector (Qiagen, Valencia, CA) for expression in bacteria.

For generation of WT, SH3 W → A mutant, ΔSH3, and SH3 dAmph, the PCR-amplified DNA fragments corresponding to WT *dAmph*, ΔSH3 *dAmph* (residues 1–522), and SH3 *dAmph* (residues 523–602) were subcloned into pDEST17 with an N-terminal His tag using the Gateway Cloning System (Life Technologies, Invitrogen, Carlsbad, CA). PCR-amplified full-length W → A *dAmph* SH3 mutant (W580→A) was synthesized using the QuikChange Site-Directed Mutagenesis Kit (Stratagene, La Jolla, CA).

Generation of HA-dAmph WT in pRmHA-3 vector for expression in S2 cells

The expressed sequence tag LD19810, representing the cDNA of Amphiphysin, was obtained from the Berkeley *Drosophila* Genome Project (Berkeley, CA). PCR-amplified full-length *dAmph* containing *Eco*RI and *Kpn*I sites was subcloned into pRmHA-3 for expression in S2 cells. An N-terminal HA tag was inserted using the QuikChange Site-Directed Mutagenesis Kit.

Mass spectrometry

Bacterially expressed, GST-tagged *dNedd4Lo* Nterm and Mid regions were lysed in sonication buffer (1× phosphate-buffered saline [PBS], 10 μg/ml aprotinin, 5 μg/ml pepstatin, 1 μg/ml leupeptin, 50 μg/ml DNase I, 1 mg/ml lysozyme, and 1 mM phenylmethylsulfonyl fluoride [PMSF]) at 4°C. Cell lysates were incubated with glutathione–Sepharose beads (Sigma-Aldrich, Oakville, Canada) for 1 h at 4°C. After incubation, beads were washed with low-salt HNTG (20 mM 4-(2-hydroxyethyl)-1-piperazineethanesulfonic acid [HEPES], pH 7.5, 150 mM NaCl, 10% glycerol, and 0.1% Triton X-100) and 1× PBS. Proteins were eluted in 1× PBS (pH 8.0) containing reduced glutathione for 1 h at 4°C (Sigma-Aldrich).

For *Drosophila* embryo collection and preparation, WT adult flies were placed on grape agar plates with yeast for embryo collection (0–24 h) at 22°C in fly cages. Approximately 300 embryos were collected and dechorionated in 50% bleach for 2 min. Embryos were lysed in RIPA buffer (% NP-40, 0.5% Na deoxycholate, 0.1% SDS, 50 mM Tris-HCl, pH 7.4, 150 mM NaCl, 10% glycerol, and 2 mM EDTA) plus protease inhibitor cocktail (Roche Complete tablet; Roche, Mississauga, Canada) on ice.

For mass spectrometry analysis of *Drosophila* embryo lysate using dNedd4Lo N-term and Mid regions, bacterially expressed and purified GST dNedd4Lo Nterm, Mid or GST control on glutathione–Sepharose beads were incubated with embryo lysates (~100 embryos) at 4°C for 2.5 h and then washed with 1× PBS. Samples were run on SDS–PAGE and Coomassie blue stained before analysis by a Thermo LTQ-Orbitrap Hybrid Mass Spectrometer (SPARC BioCentre, Hospital for Sick Children, Toronto, Canada). X! Tandem (version Cyclone, 2010.12.01.2) was set up to search the *D. melanogaster* database in order to identify the peptide fragments generated from trypsin digestion. The mass spectrometry data were analyzed using Scaffold 4.4 software (Proteome Software).

In vitro binding assays

Bacterially expressed and purified His-tagged WT dAmph, ΔSH3 dAmph, SH3 dAmph, or W → A dAmph SH3 mutant was incubated with bacterially expressed GST-dNedd4Lo Nterm at 4°C for 2 h. Supernatant was removed, and the beads were washed with low-salt HNTG, followed by 1× PBS. After SDS–PAGE, membranes were blocked and incubated with mouse anti-His (Qiagen) to detect dAmph. Mouse anti-GST antibody (Covance, Princeton, NJ) and horseradish peroxidase (HRP)–conjugated goat anti-mouse antibody (Jackson Immuno Research Labs, West Grove, PA) were used to detect bacterially expressed GST-dNedd4Lo Nterm (Supplemental Table S2).

Coimmunoprecipitation

Subconfluent *Drosophila* S2 cells, 2 ml, were transferred into six-well plates and allowed to grow for ~16 h to obtain ~90% confluency before transfection. Effectene transfection kit (Qiagen) was used to transfect FLAG-*dNedd4S* or FLAG-*dNedd4Lo* and HA-*dAmph* in pRmHa3 vectors into S2 cells using standard protocols. We transfected 0.4 μg of DNA each for dNedd4 and dAmph per well. At 24 h posttransfection, 500 μM CuSO4 was added in each well to induce expression of the transfected dNedd4 and dAmph under the metallothionein promoter. At 48 h posttransfection, cells were lysed in lysis buffer (150 mM NaCl, 50 mM HEPES, 1% Triton X-100, 10% glycerol, 1.5 mM $MgCl_2$, and 1.0 mM ethylene glycol tetraacetic acid) plus protease inhibitors (1 mM PMSF, 1 μg/ml each of aprotinin, leupeptin, and pepstatin A). DNedd4S or dNedd4Lo was immunoprecipitated with M2 anti-Flag agarose beads (Sigma-Aldrich), and the membrane was immunoblotted with anti-HA antibody (Covance). Flag-dNedd4S and dNedd4Lo were detected using M2 anti-Flag antibody (Sigma-Aldrich) and HRP-conjugated goat anti-mouse antibody (Supplemental Table S2).

Immunohistochemistry

Wandering third-instar larvae were dissected using a standard fillet preparation technique (Brent *et al.*, 2009), fixed in 4% paraformaldehyde (20 min) or Bouin solution (Sigma-Aldrich) (5 min) for staining of glutamate receptor DGluRIIA (Developmental Studies Hybridoma Bank [DSHB], Iowa City, IA) washed in PBT

(0.1% Tween-20 in PBS), and blocked (2% bovine serum albumin, 2% normal goat serum, and/or 2% donkey serum in PBT) for 1 h at room temperature before overnight incubation with primary antibodies at 4°C. See Supplemental Table S2 for antibodies and dilutions and Supplemental Table S3 for fly line crosses. Muscle segments and postsynaptic regions from muscles 6/7 were visualized using a Zeiss AxioVert 200M confocal microscope with a Zeiss objective lens set to 100× (oil imaging medium)/numerical aperture (NA) 1.4 or 63× (water imaging medium)/NA 1.3. Confocal data were acquired at room temperature with a Hamamatsu C9100-13 electron-multiplying charge-coupled device camera, and images were analyzed and deconvolved using Volocity 6.3.0 (PerkinElmer).

Analysis of postsynaptic dAmph and T-tubule architecture in Drosophila larva. Larvae were incubated overnight with rabbit anti-Amph antibody (G. Boulianne) and mouse anti-Dlg antibody (DHSB) at 4°C. The samples were incubated for 2 h with Cy3-conjugated donkey anti-rabbit (Jackson Immuno Research Labs) and Alexa Fluor 488–conjugated goat anti-mouse (Invitrogen) antibody to visualize dAmph and Dlg, respectively (Supplemental Table S2).

Colocalization of V5-dAmph and Flag-dNedd4Lo. Larvae were immunostained with M2 anti-Flag antibody and rabbit anti-V5 primary antibodies (Millipore, Temecula, CA) overnight at 4°C. The samples were incubated for 2 h with Cy3-conjugated goat anti-mouse antibody, Alexa Fluor 488–conjugated goat anti-rabbit antibody, and Alexa Fluor 647–HRP (Jackson Immuno Research Labs) to label the presynaptic region and visualized by confocal microscopy (Supplemental Table S2).

Colocalization of V5-dAmph or MYC-ΔSH3-dAmph and endogenous dNedd4. Larvae were immunostained with rabbit anti-dNedd4 (D. Rotin) and mouse anti-V5 or mouse anti-MYC primary antibodies (Millipore) overnight at 4°C. The samples were incubated for 2 h with Cy3-conjugated donkey anti-rabbit antibody and Alexa Fluor 488–conjugated goat anti-mouse antibody (Supplemental Table S2). Colocalization of dNedd4 and dAmph (V5-WT or MYC-ΔSH3) was assessed by Volocity 6.3.0 (PerkinElmer) and expressed in terms of the Pearson's *r*.

Analysis of glutamate receptors in Amph-null mutants. Larvae were immunostained with mouse anti-DGluRIIA antibody overnight at 4°C. The samples were incubated for 2 h with Alexa Fluor 488–conjugated goat anti-mouse antibody and Alexa Fluor 647–HRP (Supplemental Table S2).

Postsynaptic localization of V5-dAmph and MYC-ΔSH3 dAmph. Larvae were immunostained with mouse anti-Dlg and rabbit anti-V5 or rabbit anti-MYC primary antibodies (Millipore) overnight at 4°C. The samples were incubated for 2 h with Cy3-conjugated donkey anti-rabbit antibody, Alexa Fluor 488–conjugated goat anti-mouse antibody, and Alexa Fluor 647–HRP (Supplemental Table S2). Colocalization of Dlg and dAmph (V5-WT or MYC-ΔSH3) was assessed by Volocity 6.3.0 (PerkinElmer) and expressed in terms of Pearson's *r*.

Western blot analysis of dAmph levels in muscles

Third-instar larvae were collected (35 larvae/line, or 10 larvae for the overexpressed V5-dAmph), washed in 1× PBS, and manually homogenized in lysis buffer plus protease inhibitors (1 mM PMSF, 1 μg/ml each of aprotinin, leupeptin, and pepstatin A) and 40 μM MG132 (Selleck Chemicals, Houston, TX) and 0.2 mM chloroquine (Bioshop, Burlington, Canada) on ice. Samples were examined by Western blotting, using rabbit anti-Amph or mouse anti-V5 antibody (AbD Serotec, Raleigh, NC) and M2 anti-Flag antibody to detect dAmph and dNedd4, respectively (Supplemental Table S2). Where indicated, the amount of dAmph was determined relative to actin using Image Studio software after subtracting the background signal from *amph*-null flies.

Statistical analysis

Quantification of postsynaptic levels of dAmph in dNedd4 transgenic fly. The postsynaptic region was identified as the area demarcated by anti-Dlg immunostaining, and the intensity of endogenous or overexpressed (using V5 antibodies) dAmph in this region was measured using Volocity 6.3.0 software (PerkinElmer). The intensity of dAmph and Dlg in this region was standardized to the levels of dAmph in WT or *24B*-Gal4 flies for overexpressed V5-dAmph. For endogenous dAmph levels, the intensity of dAmph measured in *amph*-null mutants was subtracted from the intensity of dAmph measured for each sample to eliminate background signal from the dAmph antibody. Student's *t* test was performed to analyze levels of dAmph in the presence of dNedd4 isoforms and the dNedd4Lo(C→A) mutant. $p < 0.05$ was considered significant.

Quantification of defective muscle T-tubules in dNedd4Lo transgenic fly. The indicated numbers of muscle 6/7 hemisegments for *Amph-null* (28), WT (80), dNedd4S (30), dNedd4Lo (39), and dNedd4Lo(C→A) (94) were analyzed and compared with WT to determine whether segments appeared normal or abnormal. Muscle segments that showed reduced T-tubules numbers were defined as abnormal. GraphPad Prism 5.0 software (GraphPad, San Diego, CA) and Fisher's exact test in a 2 × 2 contingency table were used to analyze the data for T-tubule defects of body wall muscle segments. The T-tubules that appeared to branch from a longitudinal tubule segment were also counted double blindly. For each muscle segment analyzed, the mean T-tubules along three different longitudinal segments of a hemisegment were counted. GraphPad Prism 5.0 software and Student's *t* test were use to quantify the number of T-tubules branching along segments of longitudinal tubules.

Larval locomotor activity

The following genotypes were used to analyze larval locomotion: 1) *Drosophila* Amphiphysin heterozygous $dAmph^{5E3}$/+, 2) *Drosophila* Amphiphysin homozygous $dAmph^{5E3}/dAmph^{5E3}$ (null mutant), 3) the muscle-specific driver line *24B*-Gal4, 4) overexpression of *dNedd4Lo* in muscles, UAS-*dNedd4Lo*;*24B*-Gal4, and 5) overexpression of *dNedd4Lo* in muscles in *Drosophila* Amphiphysin heterozygous background UAS-$dNedd4Lo/dAmph^{5E3}$;*24B*-Gal4.

To ensure that all larvae were at the same physiological age, the time taken to reach the wandering third-instar stage was monitored. About equal numbers of adult flies (50 males and 50 females) were transferred to freshly prepared grape agar plates to lay eggs and housed in an environmental room at 25°C, 60% relative humidity, and 12-h light/dark cycle. After 30 h, hatched larvae were cleared from the plate, and all newly hatched larvae were collected 2 h later. These larvae were transferred into vials containing standard fly food medium. UAS-*dNedd4Lo*;*24B*-Gal4 and UAS-$dNedd4Lo/dAmph^{5E3}$;*24B*-Gal4 larvae showed delayed development, taking 170 ± 4 h after egg laying to reach the wandering stage, whereas $dAmph^{5E3}$/+, $dAmph^{5E3}/dAmph^{5E3}$, and *24B*-Gal4 larvae reached the wandering stage 158 ± 4 h after egg laying.

Video tracking and analysis of data

All behavioral experiments were performed at a 4-h time window (between 15.00 and 19.00 h) in an environmental control room (40–45% relative humidity, 25°C). Each wandering third-instar larva was taken out of the wall of the vial, washed briefly with distilled water, and gently transferred using a paintbrush to the center of a 92 × 16–mm Petri dish plate (Sarstedt, Numbrecht, Germany) containing 3% agarose. The plate was placed on a cold-light x-ray film illuminator (model 140001; S&S X-Ray Products) with a homogeneous emission. A color camera (EverFocus EQ610, Polistar II) was fitted with a CCTV lens (Computar, Vari Focal TG4Z2813 FCS-IR) and fixed on a mounting bracket ~50 cm above the plate. The distance of the camera to the object, the zoom, and the focus and iris aperture were optimized for video tracking. The path of freely crowding larvae within the arena was tracked during 2 min with Ethovioson XT, version 10 (Noldus Information Technology, Leesburg, VA). Video recording was started right after the first full wave of contraction was observed. All video recordings obtained from video tracking were saved as MPEG movies. For analysis of locomotor activity, the behavioral data were Box–Cox transformed to correct problems of distribution and nonhomogeneity of variance before transformation. Normal distribution was confirmed by the Shapiro–Wilk test. The homogeneity of variance was tested by the Levene test ($F4,169 = 2.40$, $p = 0.058$). One-way analysis of variance and subsequent Turkey post hoc comparisons were performed to evaluate differences among genotypes. Statistical analyses were conducted using Statistica 8.0 (StatSoft) software.

Morphometrics

Because the differences in larval body length may have an effect on total distance covered in a given period of time, we performed morphometric measurement in animals from all studied genotypes. The length of each larva was measured from the apex to the base. Before the measurements, ~20 larvae/genotype were placed into a container, one end of which was covered with mesh. This container was submerged into a 70°C water bath for 30 s to fix larvae in an extended state. The images were captured using the OptixCam (OCS-SK2-14X) digital camera attached to a Nikon SMZ645 stereoscope and then analyzed with ToupView 3.0. The morphological data (larval body length) were tested with a Kruskal–Wallis test. There were no significant differences between genotypes: $H(4, N = 110) = 6.832545$, $p = 0.1450$.

ACKNOWLEDGMENTS

This work was supported by the Natural Sciences and Engineering Research Council of Canada (to D.R. and G.B.). D.R. and G.B. hold Canada Research Chairs (CRC Tier I).

REFERENCES

Al-Qusairi L, Laporte J (2011). T-tubule biogenesis and triad formation in skeletal muscle and implication in human diseases. Skelet Muscle 1, 26–26.

Bao H, Reist NE, Zhang B (2008). The Drosophila epsin 1 is required for ubiquitin-dependent synaptic growth and function but not for synaptic vesicle recycling. Traffic 9, 2190–2205.

Bar-Sagi D, Rotin D, Batzer A, Mandiyan V, Schlessinger J (1993). SH3 domains direct cellular localization of signaling molecules. Cell 74, 83–91.

Bate M (1990). The embryonic development of larval muscles in Drosophila. Development 110, 791.

Baumann C, Lindholm CK, Rimoldi D, Lévy F (2010). The E3 ubiquitin ligase Itch regulates sorting nexin 9 through an unconventional substrate recognition domain. FEBS J 277, 2803–2814.

Baylies MK, Bate M, Gomez MR (1998). Myogenesis: a view from Drosophila. Cell 93, 921–927.

Brent JR, Werner KM, McCabe BD (2009). Drosophila larval NMJ dissection. J Vis Exp 24, doi 10.3791/1107.

Caldwell JL, Smith CER, Taylor RF, Kitmitto A, Eisner DA, Dibb KM, Trafford AW (2014). Dependence of cardiac transverse tubules on the BAR domain protein amphiphysin II (BIN-1). Circ Res 115, 986–996.

Collins CA, DiAntonio A (2007). Synaptic development: insights from Drosophila. Curr Opin Neurobiol 17, 35–42.

DiAntonio A, Haghighi AP, Portman SL, Lee JD, Amaranto AM, Goodman CS (2001). Ubiquitination-dependent mechanisms regulate synaptic growth and function. Nature 412, 449–452.

Di Paolo G, Sankaranarayanan S, Wenk MR, Daniell L, Perucco E, Caldarone BJ, Flavell R, Picciotto MR, Ryan TA, Cremona O, De Camilli P (2002). Decreased synaptic vesicle recycling efficiency and cognitive deficits in amphiphysin 1 knockout mice. Neuron 33, 789–804.

Dobi KC, Schulman VK, Baylies MK (2015). Specification of the somatic musculature in Drosophila. Wiley Interdiscip Rev Dev Biol 4, 357–375.

Folker ES, Baylies MK (2013). Nuclear positioning in muscle development and disease. Front Physiol 4, 363.

Glickman MH, Ciechanover A (2002). The ubiquitin-proteasome proteolytic pathway: destruction for the sake of construction. Physiol Rev 82, 373–428.

Grabs D, Slepnev VI, Songyang Z, David C, Lynch M, Cantley LC, Camilli PD (1997). The SH3 domain of amphiphysin binds the proline-rich domain of dynamin at a single site that defines a new SH3 binding consensus sequence. J Biol Chem 272, 13419–13425.

Hong T, Smyth JW, Gao D, Chu KY, Vogan JM, Fong TS, Jensen BC, Colecraft HM, Shaw RM (2010). BIN1 localizes the L-type calcium channel to cardiac T-tubules. PLoS Biol 8, e1000312.

Hong T, Yang H, Zhang S, Cho HC, Kalashnikova M, Sun B, Zhang H, Bhargava A, Grabe M, Olgin J, *et al.* (2014). Cardiac BIN1 folds T-tubule membrane, controlling ion flux and limiting arrhythmia. Nat Med 20, 624–632.

Ing B, Shteiman-Kotler A, Castelli M, Henry P, Pak Y, Stewart B, Boulianne GL, Rotin D (2007). Regulation of Commissureless by the ubiquitin ligase DNedd4 is required for neuromuscular synaptogenesis in Drosophila melanogaster. Mol Cell Biol 27, 481–496.

Landgraf M, Baylies M, Bate M (1999). Muscle founder cells regulate defasciculation and targeting of motor axons in the Drosophila embryo. Curr Biol 9, 589–592.

Landgraf M, Jeffrey V, Fujioka M, Jaynes JB, Bate M (2003). Embryonic origins of a motor system: motor dendrites form a myotopic map in Drosophila. PLoS Biol 1, E41.

Lee E, Marcucci M, Daniell L, Pypaert M, Weisz OA, Ochoa G, Farsad K, Wenk MR, De Camilli P (2002). Amphiphysin 2 (Bin1) and T-tubule biogenesis in muscle. Science 297, 1193–1196.

Leventis PA, Chow BM, Stewart BA, Iyengar B, Campos AR, Boulianne GL (2001). Drosophila Amphiphysin is a post-synaptic protein required for normal locomotion but not endocytosis. Traffic 2, 839–850.

Lichte B, Veh RW, Meyer HE, Kilimann MW (1992). Amphiphysin, a novel protein associated with synaptic vesicles. EMBO J 11, 2521–2530.

Lipsett DB, Frisk M, Singh N, Aronsen JM, Marszalec W, Sejersted OM, Sjaastad I, Wasserstrom JA, Christensen G, Louch WE (2015). Bridging Integrator 1 (BIN1) initiates T-tubule growth during cardiac development and disease. Biophys J 108, 130a.

Muller AJ, Baker JF, DuHadaway JB, Ge K, Farmer G, Donover PS, Meade R, Reid C, Grzanna R, Roach AH, *et al.* (2003). Targeted disruption of the murine bin1/amphiphysin ii gene does not disable endocytosis but results in embryonic cardiomyopathy with aberrant myofibril formation. Mol Cell Biol 23, 4295–4306.

Peter BJ, Kent HM, Mills IG, Vallis Y, Evans PR, McMahon HT (2004). BAR domains as sensors of membrane curvature: the Amphiphysin BAR structure. Science 303, 495–499.

Razzaq A, Robinson IM, McMahon HT, Skepper JN, Su Y, Zelhof AC, Jackson AP, Gay NJ, O'Kane CJ (2001). Amphiphysin is necessary for organization of the excitation-contraction coupling machinery of muscles, but not for synaptic vesicle endocytosis in Drosophila. Genes Dev 15, 2967–2979.

Rotin D, Kumar S (2009). Physiological functions of the HECT family of ubiquitin ligases. Nat Rev Mol Cell Biol 10, 398–409.

Stamenova SD, Dunn R, Adler AS, Hicke L (2004). The Rsp5 ubiquitin ligase binds to and ubiquitinates members of the yeast CIN85-endophilin complex, Sla1-Rvs167. J Biol Chem 279, 16017–16025.

Su J, Chow B, Boulianne GL, Wilde A (2013). The BAR domain of amphiphysin is required for cleavage furrow tip-tubule formation during cellularization in Drosophila embryos. Mol Biol Cell 24, 1444–1453.
Tian X, Wu C (2013). The role of ubiquitin-mediated pathways in regulating synaptic development, axonal degeneration and regeneration: insights from fly and worm. J Physiol 591, 3133–3143.
Tjondrokoesoemo A, Park KH, Ferrante C, Komazaki S, Lesniak S, Brotto M, Ko J, Zhou J, Weisleder N, Ma J (2011). Disrupted membrane structure and intracellular Ca^{2+} signaling in adult skeletal muscle with acute knockdown of Bin1. PLoS One 6, e25740.
Volk T (1999). Singling out Drosophila tendon cells: a dialogue between two distinct cell types. Trends Genet 15, 448–453.
Wan HI, DiAntonio A, Fetter RD, Bergstrom K, Strauss R, Goodman CS (2000). Highwire regulates synaptic growth in Drosophila. Neuron 26, 313–329.
Wolf B, Seeger MA, Chiba A (1998). Commissureless endocytosis is correlated with initiation of neuromuscular synaptogenesis. Development 125, 3853–3863.
Zelhof AC, Bao H, Hardy RW, Razzaq A, Zhang B, Doe CQ (2001). Drosophila Amphiphysin is implicated in protein localization and membrane morphogenesis but not in synaptic vesicle endocytosis. Development 128, 5005–5015.
Zhong Y, Shtineman-Kotler A, Nguyen L, Iliadi KG, Boulianne GL, Rotin D (2011). A splice isoform of DNedd4, DNedd4-long, negatively regulates neuromuscular synaptogenesis and viability in Drosophila. PLoS One 6, e27007.